

An RC filter for hydraulic switching control with a transmission line between valves and actuator

Rainer Haas^{a*}, Evgeny Lukachev^{a*} and Rudolf Scheidl^b

^aLinz Center of Mechatronics GmbH, Altenbergerstraße 69, 4040 Linz, Austria; ^bJohannes Kepler University Linz, Institute of Machine Design and Hydraulic Drives, Altenbergerstraße 69, 4040 Linz, Austria

(Received 31 July 2014; accepted 26 September 2014)

Hydraulic switching control with fast switching valves may excite unacceptable hydraulic and mechanical oscillations. Particularly if transmission lines are used, which have many oscillation modes, the avoidance of resonances by a proper timing of the switching pulses is hardly feasible. Then, passive filters may be a good solution. A simple RC filter applied to a cylinder drive with a transmission line to the switching valves is investigated by a transfer function analysis, numerical methods, and experiments. Properties of the dynamic behaviour are elucidated by approximate relations derived from the transfer function by asymptotic methods. A simple dimensioning rule recommends sizing the filter resistance close to the hydraulic impedance of the transmission line. The capacitance's sizing is a trade off between a potential reduction of the resonance peak due to the cylinder natural frequency and a softness of the hydraulic drive system.

Keywords: digital hydraulics; hydraulic switching control; hydraulic RC filter; pulsation attenuation

Introduction

Hydraulic switching control operates via a relatively fast and repeated switching of one or several switching valves to control states like position, speed, pressure, or force. Many different hydraulic switching circuits have been proposed and studied so far. Scheidl and Kogler (2013) give an overview about the state of the art. A simple approach, called elementary hydraulic switching control in that paper, is to replace a servo or proportional valve by switching valves. A corresponding circuit is shown in Figure 1. Some related results are reported in Scheidl *et al.* (2000) and Scheidl and Hametner (2003). Elementary switching control in contrast to switching control with an intermediate circuit means that the switching valve or valves is/are less or more directly connected to the actuator. An intermediate circuit in the context of switching control means an extra circuit of passive hydraulic components. The components can be of resistive, inductive, or capacitive nature, or check valves or even some valves with higher functionality, but which are not directly influenced by the automatic control going solely to the switching valves. They are placed between the active valves and the actuator. These intermediate circuits serve one or both of the following two purposes:

- (1) Pulsation filtering; fast switching provokes pressure and flow pulsation with a potential negative impact on the actuator motion or pressure quality and/or creates unwanted noise.
- (2) Improving efficiency; with a properly placed and dimensioned inductance element in the

intermediate circuit, flow can be taken from the low pressure line, if the actuator pressure is below the system pressure, or can be transferred to the high pressure line from the actuator; such intermediate circuits together with the switching valves are called switching converters; see, for instance Brown (1987), Brown *et al.* (1988), Kogler (2012), De Negri *et al.* (2014), and Pan *et al.* (2014).

In many applications the switching valves (V_B , V_T in Figure 1) cannot be directly mounted on the actuator, because of available space, endangering of the valves by mechanical processes in the actuator surrounding, or maintenance reasons. Then a transmission line is placed between the valve and the actuator. Such lines typically exhibit a multimodal oscillatory behaviour. It is very likely that the fast switching excites one or several of the oscillation modes which result from the coupling of the transmission line with the actuator.

In Scheidl *et al.* (2014) the authors present a simple RC hydraulic low pass filter which intends to avoid these negative transmission line effects. It is simply a hydraulic capacitance, either in form of a fluid filled cavity or in form of a usual hydraulic accumulator, and a resistance in form of a throttle. The corresponding schematic in Figure 2 shows that this RC filter is placed between the switching valves and the transmission line. Of course, the proposed RC filter is an intermediate circuit, as mentioned above. The pipeline, even though changing the dynamic response, is not an intermediate circuit according to above definition, since it does not fulfil any

*Corresponding authors. Email: rainer.haas@lcm.at (R. Haas); evgeny.lukachev@lcm.at (E. Lukachev)

sub-system, composed of the mass m and the cylinder flexibility, are disregarded. Furthermore, it contains just theoretical work without an experimental validation of the concept and the dimensioning rules.

Therefore, in the present paper, a more general theoretical study of the RC filter by a model, which includes the actuator and the multimodal transmission line dynamics, and experimental results obtained with a test rig, are presented. It also provides several analytical results based on asymptotic methods to better comprehend the dynamical behaviour of the complete system.

Mathematical system model and system evaluation

Linear system model

An analytical model of the system according to Figure 2 is based on the following simplifying assumptions, most of which just make the system linear and allow the application of linear methods for system analysis:

- The valves (V_P , V_T) are replaced by the flow rate \hat{Q}_V which they submit to the system.
- The resistance (R) and capacitance (C_H) are linear elements.

$$\frac{\hat{s}}{\hat{Q}_V} = \frac{jA_p Z_H (-j + \omega C_H R)}{\omega \left(\frac{(jm\omega - m\omega^2 C_H R - jm\omega^3 Z_H^2 C_H C_{Cyl} + j\omega Z_H^2 A_p^2) \sin(\Omega) + (jm\omega^2 (C_H + C_{Cyl}) Z_H - m\omega^3 Z_H C_H C_{Cyl} R - jZ_H A_p^2 + \omega Z_H C_H R A_p^2) \cos(\Omega)}{\omega} \right)} \quad (2)$$

- Fluid friction in the pipeline is neglected; a linear compressibility law is applied.
- The motion of the hydraulic cylinder per switching cycle is so small, that its hydraulic capacity can be considered constant over several cycles.

With these assumptions the system model is formulated in frequency domain employing the Fourier Transform (frequency ω).

$$\begin{aligned} -\omega^2 m \hat{s} &= \hat{p}_2 A_p - \hat{p}_3 A_R - \hat{F}; \quad \hat{Q}_1 = \hat{Q}_v - \hat{Q}_3 \\ \hat{Q}_3 &= (\hat{p}_1 - \hat{p}_3) / R; \quad j\omega \hat{p}_3 / C_3; \\ j\omega \hat{p}_2 &= (\hat{Q}_2 - j\omega s A_p) / C_{cyl}; \\ \hat{Q}_1 &= -j \frac{\hat{p}_1 \cos(\frac{\omega L}{c}) - \hat{p}_2}{Z_H \sin(\frac{\omega L}{c})}; \\ \hat{Q}_2 &= -j \frac{\hat{p}_2 \cos(\frac{\omega L}{c}) - \hat{p}_1}{Z_H \sin(\frac{\omega L}{c})}; \\ \hat{u}(\omega) &= \int_{-\infty}^{\infty} u(t) e^{-j\omega t} dt; \quad Z_H = \frac{\sqrt{E\rho}}{A}; \\ c &= \sqrt{\frac{E}{\rho}}; j^2 = -1; C_{cyl} = \frac{A_p s_{ref}}{E}; C_H = \frac{V_3}{E} \end{aligned} \quad (1)$$

The two transmission line equations for \hat{Q}_1, \hat{Q}_2 are, for instance, obtained as limit values of the well known transmission line model of D'Souza and Oldenburger (1964) if the viscosity goes to zero. Z_H is the hydraulic impedance of the pipeline, L its length, c the wave propagation speed of the fluid, ρ its density and E its compression modulus, s the piston position, s_{ref} its value in the reference state (for linearization), A the pipe cross section, A_p the piston area, A_R the rod sided active piston area, m the moved mass; the remaining variables can be identified from Figure 2. If the system pressure source fed to the rod sided cylinder chamber provides fairly constant pressure in the relevant frequency range, this cylinder side does not play a significant role for the filtering dynamics. Of course, it influences the pressure offset, which has effect on the linearization of the actually nonlinear elements, like an orifice to realize the resistance R or a gas filled accumulator to build the capacitance C_H . For the further it is assumed that these influences are properly considered in the respective parameters of the linear models of those elements.

From Equations (1) the frequency domain state vector $\hat{\mathbf{x}} = [\hat{s}, \hat{p}_1, \hat{p}_2, \hat{p}_3, \hat{Q}_1, \hat{Q}_2, \hat{Q}_3]$ can be computed as function of the input vector $\hat{\mathbf{u}} = [\hat{Q}_V, \hat{F}]$. This can even be done symbolically, but the expressions are very lengthy

and, therefore, are not presented. Due to problem linearity, the result is a linear combination of both components of $\hat{\mathbf{u}}$. The \hat{F} dependent part is omitted here, since we are not so much interested in the effects of a time varying load. Only the part of the solution affected by \hat{Q}_V is investigated further. The most essential state is the position s , or its Fourier transform \hat{s} , respectively. The corresponding analytical result is shown in Equation (2).

Asymptotic analysis of the linear system model

Expression (2) does not provide much direct insight, due to its complexity and the number of system parameters. Therefore, nondimensional parameters are used instead, to exploit a potential reduction of the effective number of system parameters and, furthermore, of a potential simplification by neglecting small effects represented by small nondimensional parameters. The nondimensionalization is given by the following relations.

$$\begin{aligned} \tau_{CR} &= \frac{C_H R c}{L}; \quad \Omega = \frac{\omega L}{c}; \quad \mu = \frac{\rho A L}{m}; \\ a &= \frac{A}{A_p}; \quad \lambda = \frac{s_{ref}}{L}; \quad \gamma = \frac{C_H}{C_{Cyl}} \end{aligned} \quad (3)$$

With these scales, Equation (2) transforms to Equation (4).

$$\frac{\hat{s} c A_p}{\hat{Q}_V L} = \Phi(\Omega) = \frac{1 + j \Omega \tau_{CR}}{\Omega \left(-\Omega \tau_{CR} \left(\cos(\Omega) \left(1 - \frac{a \Omega^2 \lambda}{\mu} \right) - \sin(\Omega) \frac{\Omega a^2}{\mu} \right) - j \left(\cos(\Omega) \left(\frac{a \Omega^2 \lambda (1 + \gamma)}{\mu} - 1 \right) + \sin(\Omega) \left(\frac{a^2 \Omega - \Omega^3 \lambda^2 \gamma}{\mu} + \frac{\Omega \lambda \gamma}{a} \right) \right) \right)} \quad (4)$$

μ is the mass ratio of the fluid in the pipe and the load. In many applications μ will be a rather small quantity. The data given in Table 1 – “Large Cylinder” are for a very large drive, for instance for a very large press or for the hydraulic gap control cylinder in a rolling mill. For these values, μ computes to $\mu \approx 2 \text{ E-5}$.

In case $\tau_{CR} \rightarrow \infty$ the transfer behaviour reduces to that of the system without the RC filter and reads

$$\frac{\hat{s} c A_p}{\hat{Q}_V L} = \frac{\mu j}{-\Omega (\cos(\Omega) \Omega^2 a \lambda + \sin(\Omega) \Omega a^2 - \mu \cos(\Omega))} \quad (5)$$

Its nontrivial poles are roots of the following essential part of the denominator.

$$(\Omega^2 a \lambda - \mu) = -\tan(\Omega) \Omega a^2 \quad (6)$$

Since the pipeline piston area ratio a is mostly a very small value (see the values for three cases of Table 1), two types of roots of Equation (6) exist. The first type is just one root pair $\pm \Omega_{Cyl}$ and is close to that values of Ω which make the left hand side zero, provided they do not correspond to a pole of the tangent function. They correspond to the free oscillation of the mass m in the cylinder capacitance C_{Cyl} , as Equation (7) shows.

$$\Omega_{Cyl} = \sqrt{\frac{\mu}{a \lambda}} \Leftrightarrow \omega_{Cyl} = \sqrt{\frac{A_p E}{m s_{ref}}} \quad (7)$$

A better approximation is

$$\Omega_{Cyl} = \sqrt{\frac{\mu}{a(a + \lambda)}} \quad (8)$$

which results from the assumption that $\tan(\Omega)$ can be approximated by Ω , i.e. $\tan(\Omega) \sim \Omega$, provided the root Ω_{Cyl} is sufficiently away from the poles of $\tan(\Omega)$.

The second type of roots are dominated by the transmission line. This can be easily seen for $\mu \rightarrow 0$. Then, Equation (6) has the nontrivial real poles according to Equation (9).

$$\frac{\lambda}{a} \Omega_n = -\tan(\Omega_n) \quad (9)$$

The solutions of Equations (6) and (9) are best assessed from Figure 3.

The roots of Equation (9) correspond to the free oscillations of the combined transmission line – cylinder hydraulic capacitance system. The load mass m cancels out, since this relation is valid for very small μ only. The roots are close to those of the pure transmission line with one closed and one open end. The factor λ/a is the volume ratio of hydraulic cylinder chamber in reference position s_{ref} and the transmission line. If λ/a is very large – for the data of Table 1 – “Large cylinder” it computes to 564.9 – an asymptotic expression for the n -th nontrivial root (the trivial root is $\Omega = 0$) is

$$\Omega_n = (2n - 1) \frac{\pi}{2} + \frac{2}{\pi} \frac{a}{(2n - 1) \lambda} - \frac{2^3}{\pi^3 (2n - 1)^3} \left(\frac{a}{\lambda} \right)^2 + O\left(\left(\frac{a}{\lambda} \right)^3 \right); \quad n \geq 1 \quad (10)$$

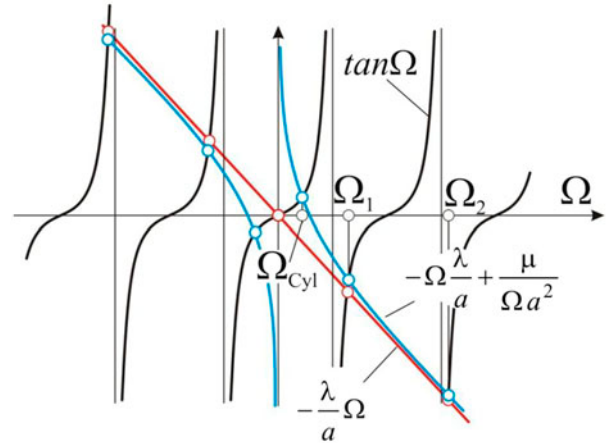


Figure 3. Graphical representation of the solutions of (6) and (9), respectively.

$$\frac{\hat{s} c A_p}{\hat{Q}_V L} \approx \frac{\mu j \Omega}{\Omega^2 a (\cos(\Omega) (a \lambda \Omega^2 - \mu) + \sin(\Omega) a^2 \Omega) + \frac{j \sin(\Omega) \lambda \gamma (a^2 \Omega^4 \lambda^2 + a^4 \Omega^2 - 2 a \lambda \mu \Omega^2 + \mu^2)}{\tau_{CR} (a \Omega^2 \lambda - \mu)}} \quad (11)$$

For a filter with a large value of τ_{CR} a corresponding asymptote for the transfer function (4) can be computed. Such an asymptote, however, if it is just computed as a formal asymptotic expansion in τ_{CR} at infinity, would have a leading term with poles at the frequencies Ω_n according to Equation (10). More appropriate is to approximate the denominator by the sum of the real-part plus the imaginary part at the zeros of the real part (for $\mu = 0$ these are the Ω_n according to Equation (10)) and take just the leading term of the numerator with respect to τ_{CR} . This leads to Equation (11).

A good estimate for the extreme values at the poles at Ω_n of the amplitude of Equation (11) for small μ is therefore

$$\max_n \left(\frac{\hat{s} c A_p}{\hat{Q}_V L} \right) \approx \frac{\mu \tau_{CR}}{\sin(\Omega_n) \gamma \Omega_n (\lambda^2 \Omega_n^2 + a^2)} \quad (12)$$

Approximations of Ω_n , which are roots of the real part of the denominator term of the transfer function (11), are given by Equation (10). The largest nontrivial value (besides the pole at $\Omega = \Omega_{Cyl}$) will be for $n = 1$. Inserting Equation (10) in Equation (12) gives the following lowest order approximation in a/λ .

$$\max \left(\frac{\hat{s} c A_p}{\hat{Q}_V L} \right) \approx \frac{8\mu \tau_{CR}}{\lambda^2 \pi^3 \gamma} \quad (13)$$

An approximation of the transfer function at the special pole $\Omega = \pm\Omega_{Cyl}$ is derived on basis of the following assumptions: a and μ are small, γ and λ are $O(1)$ and, furthermore, $\mu \leq a$. Then Ω_{Cyl} is also $O(1)$ and justifies the following simplification of Equation (4) at that pole for large values of τ_{CR} .

$$\left. \frac{\hat{s} c A_p}{\hat{Q}_V L} \right|_{\Omega=\Omega_{Cyl}} \approx -\frac{\tau_{CR}}{\gamma \cos(\Omega_{Cyl})} \quad (14)$$

Besides these maximum responses of the system to an excitation by Q_{js} a second important criterion of the RC filter is the oscillatory behaviour of the autonomous system reflected by its natural frequencies and damping properties. Both are given by the poles of the transfer function, i.e. the zeros of the denominator. For large τ_{CR} an approximation of the natural frequencies is given by Equations (6) and (9), respectively. The damping corresponds to the imaginary parts of Ω . For comprehensive analytical results, an asymptotic solution with respect to

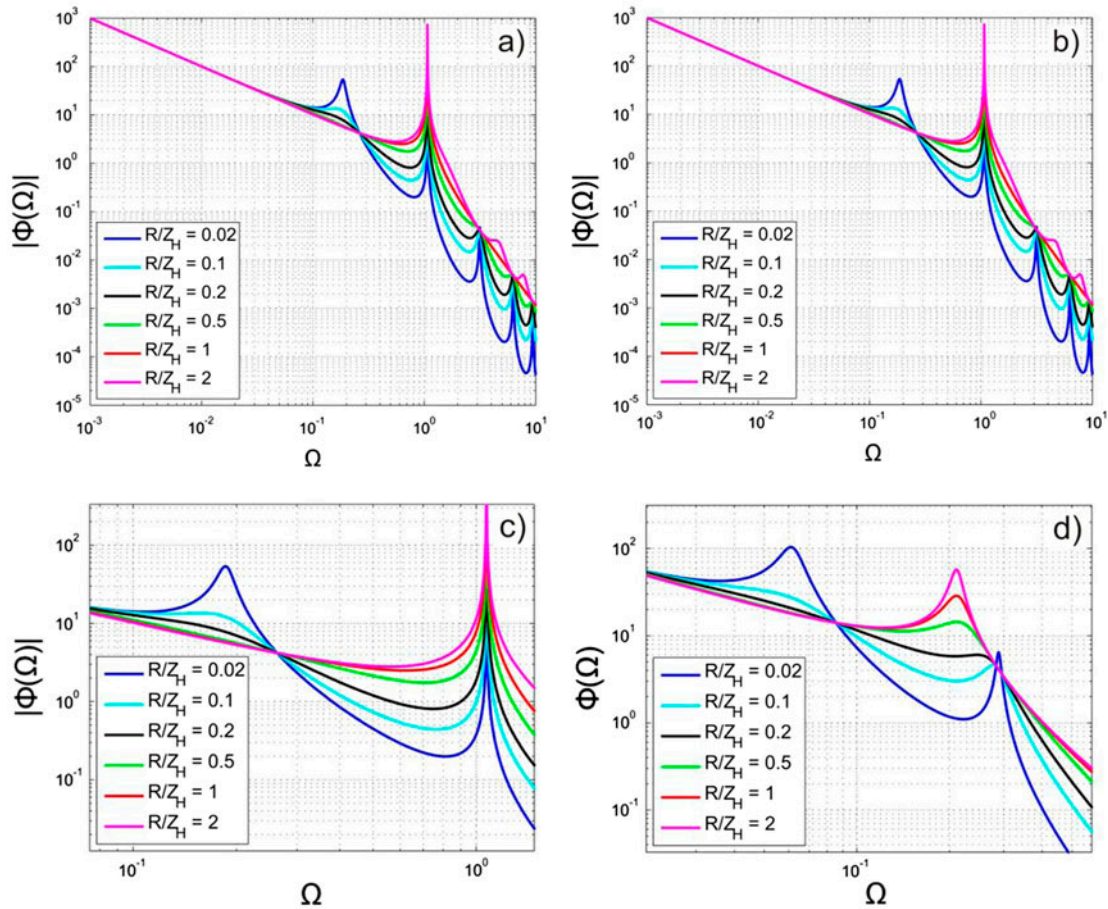


Figure 4. Amplitude plot of $\Phi(\Omega)$ (according to (4)) for different values of R/Z_H ; (a) and (c): parameters of large cylinder case according to Table 1; (b) and (d): parameters of small cylinder case according to Table 1; (c) and (d) are zoomings of the resonance peaks at $\Omega = \Omega_{Cyl}$ of (a) and (b). The first (leftmost) pole is at $\Omega = \Omega_C$ (it exists only for $\tau_{CR} < \tau_{CR,apl}$), the second at $\Omega = \Omega_{Cyl}$, the others at $\Omega = \Omega_n$.

large τ_{CR} is derived. To this end the roots are expressed as series in $1/\tau_{CR}$.

$$\Omega = \Omega_R + j\Omega_I; \quad \Omega_R = \sum_{i=0}^{\infty} \Omega_{R,i} \tau_{CR}^{-i}; \quad \Omega_I = \sum_{i=1}^{\infty} \Omega_{I,i} \tau_{CR}^{-i} \quad (15)$$

$$\begin{aligned} & (\mu^2 + \mu a^2 + a^4 \Omega_{R,0}^2 + \lambda^2 a^2 \Omega_{R,0}^4 + a^3 \lambda \Omega_{R,0}^2 - 2a\lambda\mu \Omega_{R,0}^2) \Omega_{R,1} = 0 \\ \cos(\Omega_{R,0}) & \left(\begin{array}{l} \Omega_{I,1}(a^5 \Omega_{R,0}^2 + a^4 \lambda \Omega_{R,0}^2 + a^3 \lambda^2 \Omega_{R,0}^4 - 2a^2 \lambda \mu \Omega_{R,0}^2 + a\mu^2 + a^3 \mu) \\ - \lambda \gamma \mu^2 - a^2 \lambda^3 \gamma \Omega_{R,0}^4 + 2a\lambda^2 \mu \Omega_{R,0}^2 - a^4 \lambda \gamma \Omega_{R,0}^2 \end{array} \right) = 0 \end{aligned} \quad (16)$$

Inserting these series into the denominator term of Equation(4) and expanding it in a power series in $1/\tau_{CR}$, gives as lowest order ($O(\tau_{CR})$) relation the real part of the denominator of Equation (4), only Ω replaced by $\Omega_{R,0}$. For small μ the solutions for $\Omega_{R,0}$ are identical to those of Equations (6) or (9), respectively. The $O(1)$ expression has a real and imaginary part. After factorization and neglect of trivial factors the two equations (see (16)) representing the real and imaginary part remain.

Equations (16) have the following results for the order one coefficients.

$$\Omega_{R,1} = 0 \quad (17)$$

$$\Omega_{I,1} = \frac{\lambda \gamma}{a} \frac{\mu^2 + \Omega_{R,0}^2 (a^2 \lambda^2 \Omega_{R,0}^2 - 2a\lambda\mu + a^4)}{a^2 \lambda^2 \Omega_{R,0}^4 + (a^4 + a^3 \lambda - 2a\lambda\mu) \Omega_{R,0}^2 + a^2 \mu + \mu^2}$$

Equations (17) tell that damping is of order $O(1/\tau_{CR})$, and the natural frequencies deviate from those of the system without filter ($\tau_{CR} \rightarrow \infty$) with $O(1/\tau_{CR}^2)$. Furthermore, damping grows with larger γ , in other words, with a larger filter capacitance C_H . If a and μ are very small values of comparable size the terms a^4 , $a^3 \lambda$, $a^2 \mu$, can be neglected in (17) and $\Omega_{I,1}$ becomes $\lambda \gamma / a$. This value is the ratio of the filter and pipeline hydraulic capacitances as Equation (18) shows.

$$\lambda \gamma / a = \frac{EC_H}{L A} = \frac{C_H}{C_{Pipe}}; \quad C_{Pipe} = \frac{L A}{E} \quad (18)$$

The Fourier transform may have imaginary eigenvalues with corresponding aperiodic behaviour. Setting $\Omega = j \delta$ the following equation for δ arises for $\mu \rightarrow 0$.

$$\begin{aligned} & \tau_{CR}(a\lambda\delta^2 \cosh(\delta) + a^2 \delta \sinh(\delta)) \\ & = a\lambda(1 + \gamma) \delta \cosh(\delta) + (a^2 + \lambda^2 \gamma \delta^2) \sinh(\delta) = 0 \end{aligned} \quad (19)$$

A closed form solution for δ cannot be found; but τ_{CR} can be easily expressed as function of δ . A representation of this function as a series in δ reads.

$$\tau_{CR} = \frac{\lambda \gamma}{a} + \frac{1}{\delta} + O\left(\frac{1}{\delta^2}\right) \quad (20)$$

$\tau_{CR,apl} = \frac{\lambda \gamma}{a}$ is the aperiodic limit. According to the monotonic nature of all terms in the series (20) only one real value for δ can exist. Physically this eigenvalue corresponds to a specific pressure compensation process, if the accumulator pressure and the static pressure according to the load do not agree. For $\tau_{CR} < \tau_{CR,apl}$ no aperiodic solution exists. $\tau_{CR,apl}$ is a remarkable choice

for τ_{CR} in the sense that for $\tau_{CR} \geq \tau_{CR,apl}$ the transfer functions own also one non oscillatory mode of the free vibrations of the system. If $\tau_{CR,opt}$ is expressed in physical parameters using the scaling relations (3) it transforms into the following condition for the resistance R .

$$R = \frac{\sqrt{E\rho}}{A} = Z_H \quad (21)$$

Equation (21) is the condition for a reflection-free terminator resistor for a transmission line with impedance Z_H . The mode corresponding to the eigenvalue δ has its origin in the RC filter, i.e., it does not exist without that filter.

For $\tau_{CR} < \tau_{CR,apl}$ an oscillatory mode occurs. An approximate formula of its frequency can be derived with physical reasoning in combination with the smallness assumptions of the parameters a and μ . An undamped pole can be expected for $\tau_{CR} \rightarrow 0$. Therefore, the denominator of $\Phi(\Omega)$ is evaluated for that case and quadratic and higher-order binomial terms of a and μ are neglected. This gives the following equation.

$$\lambda \gamma \Omega_C \tan \Omega_C = a \Rightarrow \Omega_C \approx \sqrt{\frac{a}{\lambda \gamma}} \quad (21)$$

It is the frequency of the oscillator formed by the pipe inductance ($\rho L/A$) and filter capacitance (C_H).

Figure 4 shows two graphical representations of the transfer function $\Phi(\Omega)$ for a large and a small cylinder (data according to Table 1). A resonance peak occurs close to $\Omega = \Omega_{Cyl}$. For $R = Z_H$ (aperiodic limit case, $\tau_{CR} = \tau_{CR,apl}$) no resonances of the pipeline arise. Values of τ_{CR} below the aperiodic limit $\tau_{CR,apl}$ cause a reduction of the oscillations dominated by the transmission line dynamics in a wide range and, for the small cylinder case, also of the oscillation dominated by the cylinder resonance ($\Omega = \Omega_{Cyl}$). At several distinct frequencies, the amplitudes reach those of the aperiodic limit case. These frequencies correspond to standing pressure waves in the transmission line having a node at the valve sided end. The flow rate pulsations of these frequencies are just

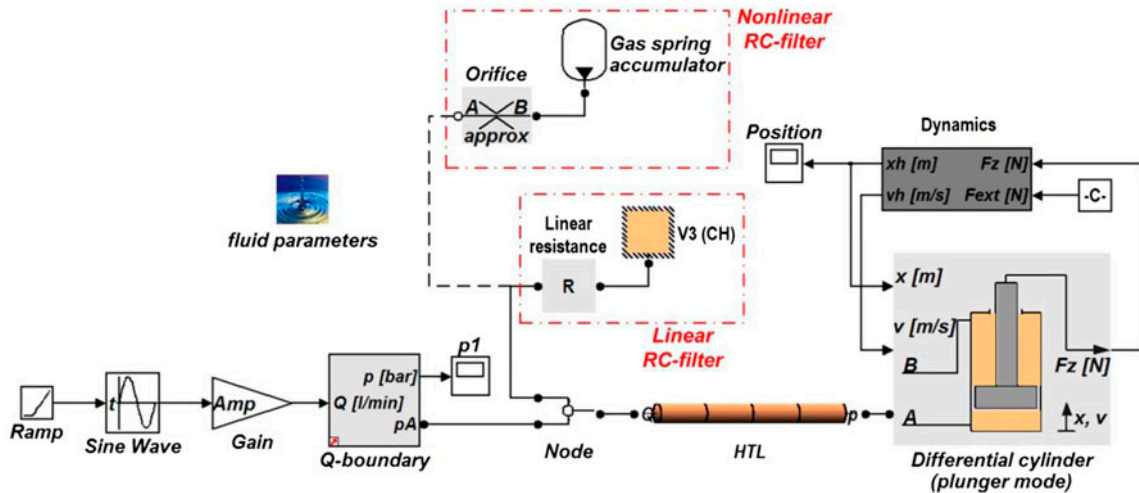


Figure 5. Schematic of the Simulink models, one with a linear RC filter, one with a nonlinear RC filter. The parameters of the components are those of Table 1 – “Test rig.” The transmission line model used a method of characteristics with a fluid friction model according to Zielke (1968).

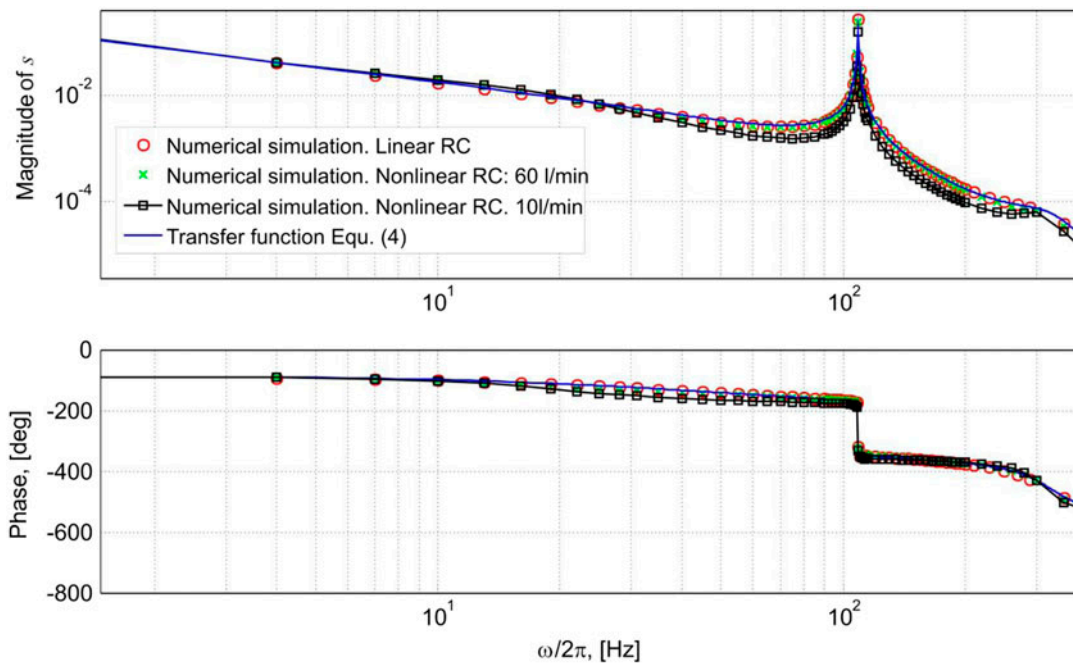


Figure 6. Steady state response oscillation amplitude and phase of the piston position s of Simulink models with linear and nonlinear RC filter compared to the analytical results using the transfer function Equation (4) as response to a sinusoidal flow rate input with amplitudes of 10 l/min and 60 l/min. For the 60 l/min amplitude the nonlinear RC model shows negligible deviations from the linear model; also in the 10 l/min case, the differences are small.

covered by the corresponding flow input harmonics, the RC filter has no effect for these frequencies because of the pressure node at its port. For a large cylinder capacity these frequencies represent $\frac{1}{2}, 1, 1\frac{1}{2}, 2, \dots$ wavelengths situations of the transmission line. Somewhat higher amplitudes (resonances) arise at $\Omega = \Omega_C$; this is the natural frequency of the oscillator formed by the capacitance C_H in combination with the inertias of the transmission line and of the piston mass m .

For $R > Z_H$ ($\tau_{CR} > \tau_{CR,apl}$) the resonance peaks at $\Omega = \Omega_C$ do not exist, since the corresponding pole δ of $\Phi(\Omega)$ is just imaginary. Transmission line dynamics-related resonance peaks occur. They constitute $\frac{1}{4}, \frac{3}{4}, \dots$ wavelengths standing waves. Also the cylinder mass system exhibits a resonance peak at $\Omega = \Omega_{Cyl}$. In the large cylinder case the RC filter cannot reduce this peak if the resistance R stays above $Z_H/10$. Smaller resistances could help but at the cost of rising amplitude of the C_H -related

oscillations ($\Omega = \Omega_C$). For the small cylinder situation, however, the RC filter can also reduce that peak. The reason is the influence of the capacitance ratio γ according to the estimate (14); γ is 5 for the small cylinder data but only 0.05 for the large cylinder data.

This finding provides a dimensioning rule for γ or rather the capacitance C_H . A larger value reduces the resonance peak but it makes also the system softer by shifting the capacitance-related mode to lower frequencies according to (22). First, it is a matter of the control bandwidth (Ω_0) how large C_H can be made to keep all system resonance out of that range ($\Omega_C > \Omega_0$). Second, also technical aspects of realizing large capacitances have to be taken into account.

A dimensioning rule for both RC design parameters, R and C_H , should consider the following general objectives:

- (1) Reduce transmission line-related oscillations.
- (2) Reduce $\Phi(\Omega_{Cyl})$.
- (3) Keep the frequency Ω_C beyond an acceptable value.
- (4) Keep the oscillations at $\Omega = \Omega_C$ below an acceptable level.

Since there are just two design parameters (R , C_H) but four objectives, the dimensioning is a trade-off problem. In the dimensioning also the controller and the relevant operation scenarios (use cases) should be taken into account. The role of R is much clearer than of C_H , as the “Small-” and “Large Cylinder” cases indicate. The authors suggest the following first guesses only as a starting point for a parameter optimization which takes the controller and the relevant operating scenarios into account:

- (1) First guess for resistance: $R = 0.5 Z_H$
- (2) First guess for $C_H = 0.5 C_{Cyl}$.

Response to a pulse input

This paper is devoted to switching control. Therefore, the system excitation happens by a single or by multiple flow rate pulses. Two extreme cases are studied analytically. A single-pulse input with three different shapes and periodically submitted pulses. The pulse shapes are: rectangular, trapezoidal, and sinusoidal. Their characteristic parameters and the corresponding Fourier Transforms are shown in Table 2.

Short pulses have a broad spectrum. Each single pulse has a countable number of zeros in its excitation spectrum. The major part of signal intensity is covered by the central part ending with the first zero ($|\Omega| = 2\pi, \approx 2.5\pi, = 3\pi$). For the sinusoidal and the trapezoidal signal the intensity decays with $1/\Omega^2$, but only with $1/\omega$ for the rectangular signal. The input signal spectrum multiplied with the transfer function (2) yields the response spectrum of the cylinder position s .

For a typical pulse width of $T_P = 10$ milliseconds, frequencies in the range of up to 600 or 900 Hz are excited. Shorter pulses have an even higher excitation bandwidth. For the drive configurations of Table 1- “Large cylinder” and “Small cylinder” cases the cylinder frequencies Ω_{Cyl} are 108.6 Hz and 100.2 Hz. Therefore, they are excited by a single pulse of the mentioned bandwidth. The RC filter can attenuate the corresponding oscillations according to the estimate (14), which is significant in the small cylinder case, as has been pointed out already before. The oscillations related to the transmission line modes, however, can be suppressed quite effectively.

Numerical models for the linear and nonlinear system

In order to check the validity of the analytical results and to study the influence of nonlinear RC components, numerical models in Matlab/Simulink using the hydraulic elements library Hydrolib3 (2014) have been set up. One model uses only linear elements for the RC system. The transmission line model employs the method of characteristics with frequency dependent damping model according to Zielke (1968) and Suzuki (1991). The other model replaces the linear resistor by an orifice with a quadratic flow rate – pressure drop relation and the linear hydraulic capacitance by a gas spring-type accumulator model with polytropic state equation. A schematic of both Simulink models is depicted in Figure 5.

In Figure 6 amplitude and phase of the transfer function (4) are compared with numerical results of the linear Simulink model showing the computed steady state results of the cylinder position to a pure sinusoidal flow

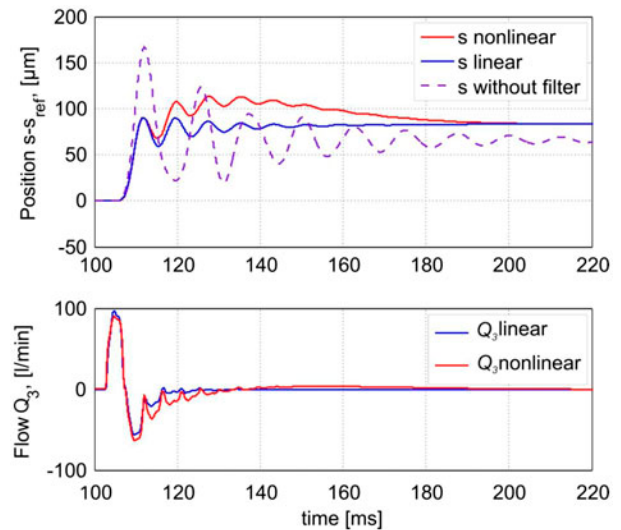


Figure 7. Response of the system with linear and nonlinear RC filter on a single pulse input; piston position s and flow rate Q_3 through the orifice are shown; parameter values are those of Table 1- “Test rig,” apart from R : linear: $R = 0.5 Z_H$; nonlinear: orifice nominal flow rate $Q_{N,orifice} = 24.5$ l/min @ 5bar; note: $Q_3 \equiv 0$ for the system without filter!

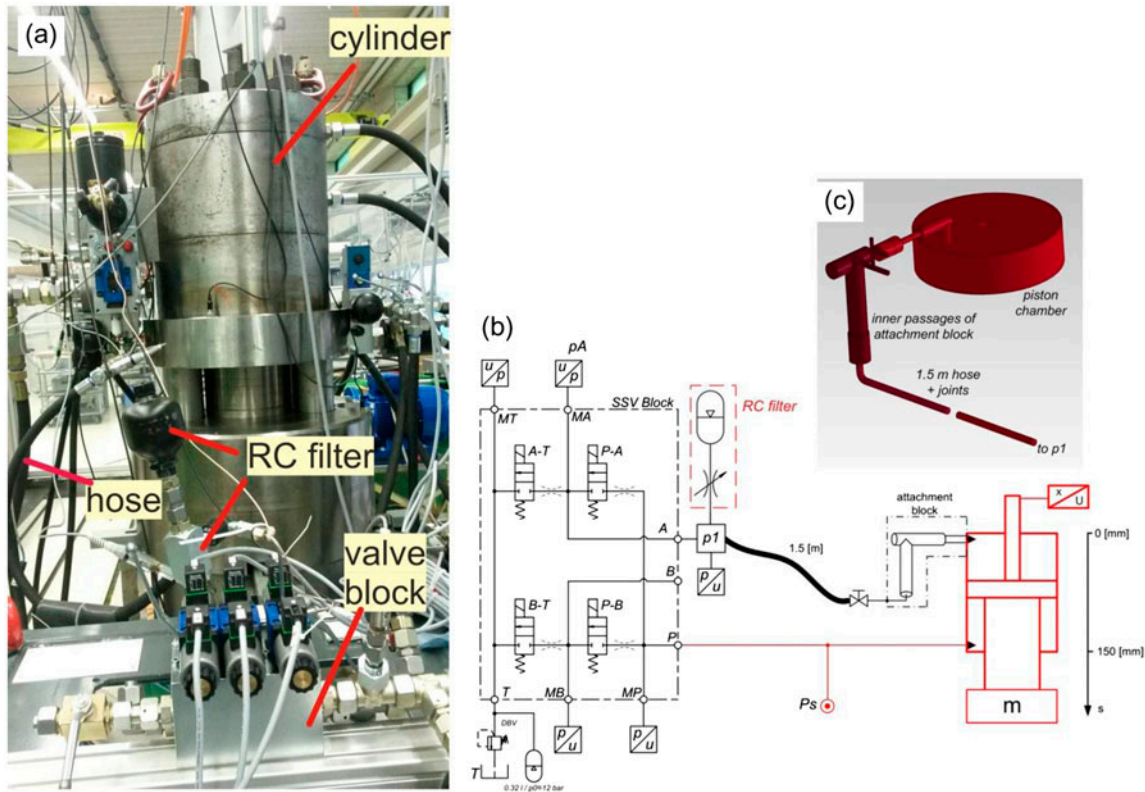


Figure 8. Digital hydraulic control test rig, photo (a) and schematic (b); data of the test rig are given in Table 1 – “Test rig.” This rig serves various purposes with two complex hydraulic blocks attached to it; these blocks have a complex bore structure (see the drawing c) which influences the dynamics of the system; in the tests presented in Figure 9 other valves (actually Rexroth WES) than shown in (a) – (Rexroth SEC) were used. The hose length indicated in (b) is shorter than the transmission line length used for computations according to Table 1 – “Test rig.” The difference is made up by the drillings in the blocks (valve block and block attached to the hydraulic cylinder) and in the thick wall of the hydraulic cylinder.

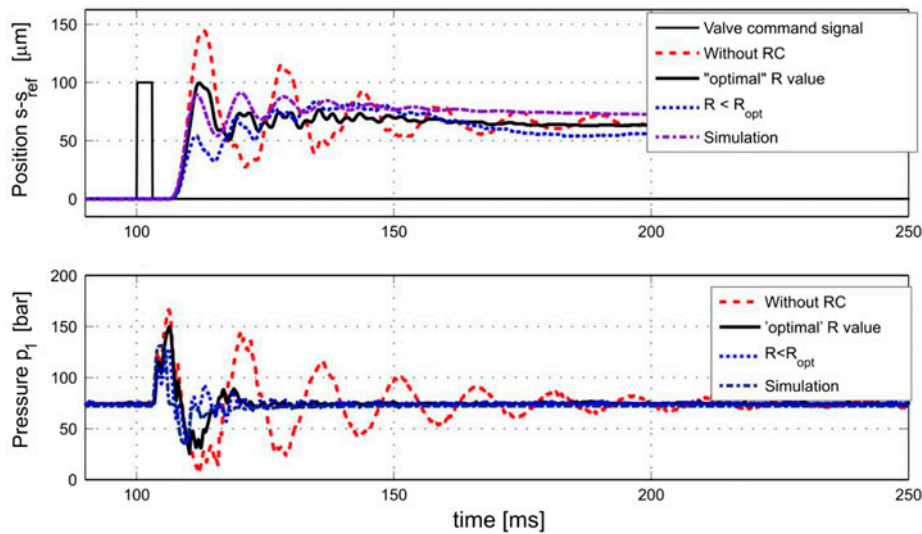


Figure 9. Piston position s and pressure p_1 after valve of experimental tests with and without RC filter and comparison with simulation results; data of the test rig according to Table 1 – “Test rig”; settings for the simulation model: command signal to valve 3 ms pulse, (nominal flow rate of valve: 45 l/min @ 5 bar; switching time: 1.9 ms, of which 1.3 ms are used to overcome valve metering edge overlap; thus hydraulic opening time is 0.6 ms); p_s : 200 bar, p_1 : 20 bar; a reduced compression modulus of $E = 10\,145$ bar was used to account for hose flexibility.

Table 1 Exemplary system parameters for three cases.

DIMENSIONAL PARAMETERS				Large cylinder	Small cylinder	Test rig
Fluid compression modulus	E	bar		14,000	14,000	12,000
Fluid density	ρ	kg/m ³		860	860	860
Mass	m	kg		15,000	150	1500
Piston area	A_p	m ²		1.000	0.010	0.096
Piston reference position	s_{ref}	m		0.2	0.2	0.1
Hydraulic capacity RC element	C_H	m ³ /Pa		7.143E-12	7.143E-12	2.143E-11
Area cross section line	A	cm ²		1.77	1.77	2.01
Length line	L	m		2.00	2.00	2.60
Hydraulic capacity cylinder	C_{Cyl}	m ³ /Pa		1.429E-10	1.429E-12	8.000E-12
Impedance line	Z_H	kg/m ⁴		6.199E+09	6.199E+09	5.054E+09
Wave speed of fluid	c	m/s		1,276	1,276	1,181
NONDIMENSIONAL PARAMETERS						
Mass ratio	line/mass	μ	-	2.030E-05	2.030E-03	2.996E-04
Area ratio	line/piston	a	-	1.770E-04	1.770E-02	2.094E-03
Length ratio	Cylinder/line	λ	-	0.100	0.100	0.038
Hydr. capacity ratios	Cylinder/line	λ/a	-	564.97	5.65	18.37
	RC/cylinder	γ	-	0.050	5.000	2.679
FREQUENCIES						
Nondimen. cyl. natur. frequ. (Equ. (7))		Ω_{Cyl}	-	1.071	1.071	1.929
Idem, better approximation (Equ. (8))		$\tilde{\Omega}_{Cyl}$	-	1.070	0.987	1.878
Cylinder natural frequency		ω_{Cyl}	rad/s	683	683	876
		f_{Cyl}	Hz	109	109	139
Ω_n accord.						
Equ. (10)	$n = 1$	Ω_1	-	1.57	1.67	1.60
	$n = 2$	Ω_2	-	4.70	4.73	4.71
	$n = 3$	Ω_3	-	7.83	7.85	7.84
Correspond. dimensional values	$n = 1$	ω_1	rad/s	1,000	1066	727
	$n = 2$	ω_2	rad/s	2,997	3020	2139
	$n = 3$	ω_3	rad/s	4,995	5009	3560
Correspond. values in Hertz	$n = 1$	f_1	Hz	159	170	116
	$n = 2$	f_2	Hz	477	481	340
	$n = 3$	f_3	Hz	795	797	567
FURTHER PARAMETERS						
Nondimen. natural frequency		Ω_C	-	0.188	0.188	0.143
Correspond. dimensional value		ω_C	rad/s	120.03	120.03	64.77
Correspond. value in Hertz		f_C	Hz	19.1	19.1	10.3
Nondimen. characteristic time	R/ZH = 1	τ_{CR}	-	28.25	28.25	49.20
	R/ZH = 0,02	τ_{CR}	-	0.565	0.565	0.984
APERIODIC LIMIT						
Hydr. capacity ratio	$a\gamma/\lambda$	$\tau_{CR,apl}$		28.25	28.25	49.20

rate input (amplitude 60 l/min and 10 l/min) for different discrete frequencies.

Figure 7 shows the response of the nonlinear and the linear models for a single pulse input for the indicated parameter settings. Two plots depict the cylinder position and flow through the throttle. At the beginning, both responses are almost the same. However when the flow Q_3 decreases the system with nonlinear elements exhibits underdamped behaviour. This stems from the low effective damping of the orifice at small flow rates compared to the derived values for the linear resistance. Nonetheless, the oscillations of the nonlinear RC filter are drastically lower than of the system without filter.

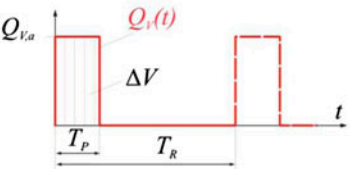
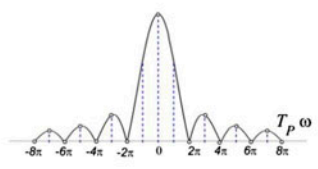
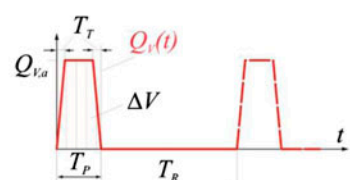
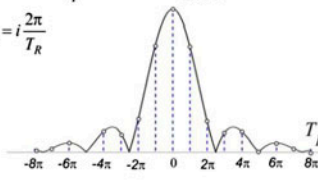
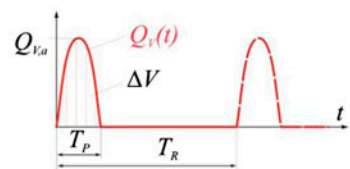
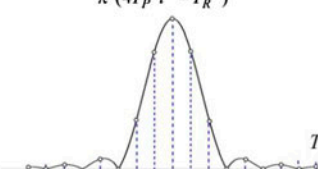
Experimental results

A test rig in the authors' hydraulic lab with a large cylinder drive for switching control is shown in Figure 8. The

hydraulic circuit corresponds basically to the schematic in Figure 2. The transmission line is formed by a hose. The RC filter is composed of a diaphragm accumulator and a throttle valve. The data of the test rig are given in Table 1. Tests with a single pulse for different settings of the RC filter have been carried out to prove the effect of the filter and of the adjustment rules derived in Section 2.2.

Figure 9 shows measured responses of the piston position and of the pressure after the valve with and without an RC filter. The "optimal" tuning of the orifice corresponds roughly to a value approximately 70% of the reflection free end resistance in case of a flow rate of 60 l/min. Exact values cannot be given, since an adjustable orifice valve was used with a relative scale. The suboptimal tuning ($R < R_{opt}$) was approximately 30% of the optimal setting. In that case the system exhibits a clear resonance due to the capacitance ($\Omega = \Omega_C$) leading to a soft oscillation with a low frequency. The overshoot due to the pole

Table 2. Shape and spectra (qualitative) of single and periodic input pulses; full lines denote single pulse, dashed lines periodic pulses; for the periodic pulses spectra shown: $T_p = T_R/2$; for the trapezoidal pulse: $T_T = T_P/5$.

Pulse shapes	Fourier spectra
<p>rectangular</p> 	$\hat{Q}_V = Q_{V,a} i \frac{e^{-iT_P \omega} - 1}{\omega}$ $\hat{Q}_{V,j} = Q_{V,a} i \frac{e^{-iT_P \omega_i} - 1}{i\pi} ; \omega_i = i \frac{2\pi}{T_R}$ 
<p>trapezoidal</p> 	$\hat{Q}_V = Q_{V,a} \frac{e^{-iT_T \omega} - e^{-iT_P \omega} + e^{-i(T_P - T_T) \omega} - 1}{T_T \omega^2}$ $\hat{Q}_{V,j} = Q_{V,a} \frac{T_R}{T_T} \frac{e^{-iT_T \omega_i} - e^{-iT_P \omega_i} + e^{-i(T_P - T_T) \omega_i} - 1}{2\pi^2 i^2}$ $\omega_i = i \frac{2\pi}{T_R}$ 
<p>sinusoidal</p> 	$\hat{Q}_V = Q_{V,a} \frac{T_P (1 + e^{-iT_P \omega})}{\pi^2 - T_P^2 \omega^2}$ $\hat{Q}_{V,j} = Q_{V,a} \frac{T_R T_P (1 + e^{-iT_P \omega_i})}{\pi (4T_P^2 i^2 - T_R^2)}$ 

at ($\Omega = \Omega_{Cyl}$), however, is less pronounced than for the ‘optimal’ setting. The proper functioning of the filter and of the tuning rule of the resistance element are clearly confirmed. Also the imperfect attenuation at lower amplitudes due to the nonlinear resistance property of the orifice is as expected and predicted by the nonlinear model. A simulation result using the nonlinear model described in a previous section is shown for comparison. The data of this model have been tuned for a good agreement, primarily by adjusting the length of the transmission line, the bulk modulus of the fluid therein, and a reduced thickness its flexible wall, to account for the compliance of the hose. Nevertheless, there is some deviation caused by the complex structure of the block attached to the hydraulic cylinder (see Figure 8c). A much more complex model would be needed for a better match. Since the purpose of the paper is showing the effect of the RC filter and not the accurate modelling of a certain hydraulic system, this complex model is not considered, particularly also because the robustness of the RC filter with respect to small system modifications should be demonstrated.

Conclusion and outlook

The proposed RC filter can attenuate oscillation coming from a transmission line between the switching valves and the hydraulic cylinder in a hydraulic switching drive. If the resistor is a linear element, it can fully annihilate all transmission line-related oscillations if its value equals the hydraulic impedance of the line. Smaller resistance values improve the attenuation at higher system frequencies but cause an additional resonance in form of a combined oscillation of the transmission line and the accumulator.

The RC filter may attenuate also the oscillations related to the cylinder attached mass system. This requires that the capacitance of the filter must be at least in the order of the cylinder.

Due to the nonlinearity of an orifice as resistance element the attenuation performance depends on the oscillation amplitude. Since the resistance of usual hydraulic throttles with a linear characteristic depend on fluid viscosity and, in turn, on fluid temperature, such throttles are not a real alternative for the orifice. As long as no

linear resistance element with a viscosity independent linear characteristic is available, the deficiencies of the throttle must be accepted. It should be mentioned that the realization of such linear throttles has been a subject of research, see e.g. Hayward (1976) and White *et al.* (1984). But these throttles employ moving mechanical components with a corresponding dynamical response behaviour which needs to be adjusted to the required bandwidth of the filter.

The RC filter is employed in ongoing research projects for digital hydraulic drives. As found in the analysis it can suppress resonance frequencies of the hydraulic cylinder if those have relatively small hydraulic capacitance. This will be tested experimentally in the future. The usefulness of the RC filter in the reduction of some oscillation problems in switching control encourages analyzing other filters too. In hydraulic switching converters which aim at improved energy efficiency resistance elements potentially deteriorate the efficiency. Therefore filters without a dissipative element should be used. Such filters will be another subject of further research.

Nomenclature

A	Area cross-section of transmission line	A_p, A_R	Piston areas
C_H, C_{Cyl}	Hydraulic capacities of RC Element and cylinder chamber	E	Fluid compression modulus
F, \hat{F}	Load force and its Fourier transform	L	Length of transmission line
Q_1, Q_2	Flow rates	\hat{Q}_1, \hat{Q}_2	Fourier Transform of flow rates
Q_3, Q_V $Q_{V,a}$	Input flow rate amplitude	\hat{Q}_3, \hat{Q}_v R	Linear hydraulic resistance
T_B, T_R, T_T	Characteristic times of input pulses	Z_H	Hydraulic impedance of transmission line
a	Area ratio of transmission line and piston	c	Wave propagation speed
j	Imaginary unit	m	Mass attached to piston
n	Order of natural frequency of the system	$p_1, p_2,$ p_3	Pressures
$\hat{p}_1, \hat{p}_2, \hat{p}_3$	Fourier Transform of pressures	\hat{p}_s	System pressure
s, s_{ref}	Piston position, reference value	t	Physical time
$\hat{\mathbf{u}}$	Fourier transform of input vector	$\hat{\mathbf{x}}$	Fourier transform of state vector
Φ	Nondimensional Transfer function: piston position over input flow rate	Ω	Nondimensional Fourier frequency

Ω_C	Nondimensional natural frequency dominated by the transmission line inductance and RC filter capacitance	Ω_n	n-th order nondimensional natural frequency dominated by the transmission line eigenmodes
$\Omega_R, \Omega_I, \Omega_{R,i}, \Omega_{I,i}$	Real and imaginary part eigenvalues of the transfer function and their i-th component of an asymptotic expansion in τ_{CR}	γ	Capacitance ratio of RC filter and cylinder chamber
δ	Absolute value of a purely imaginary Ω	μ	Mass ratio of transmission line fluid and mass m
λ	Length ratio of piston reference position and transmission line	τ_{CR}	Nondimensional characteristic time of RC filter
ρ	Fluid density	ω_{Cyl}	Natural frequency of the system dominated by the cylinder – mass system
ω	Fourier frequency		

Acknowledgement

This work has been carried out at LCM GmbH as part of a K2 project. K2 projects are financed using funding from the Austrian COMET-K2 programme. The COMET K2 projects at LCM are supported by the Austrian federal government, the federal state of Upper Austria, the Johannes Kepler University and all of the scientific partners which form part of the K2-COMET Consortium.

References

- Brown, F.T., 1987. Switched reactance hydraulics: a new way to control fluid power. *In: National conference on fluid power*. Chicago: NFPA, 25–34.
- Brown, F.T., Tentarelli, S.C., and Ramachandran, S., 1988. A hydraulic rotary switched-inertance servo-transformer. *ASME Journal of Dynamic Systems, Measurement, and Control*, 110 (2), 144–150.
- D'Souza, A. and Oldenburger, R., 1964. Dynamic response of fluid lines. *ASME, Journal of Basic Engineering*, 86, 589–598.
- De Negri, V.J., *et al.*, 2014. Behavioural prediction of hydraulic step-up switching converters. *International Journal of Fluid Power*, 15 (1), 1–9.
- Edge, K.A. and Johnston, D.N., 1990a. The secondary source method for the measurement of pump pressure ripple characteristics. Part 1 – Description of Method. *Proceedings of the Institution of Mechanical Engineers, Part I: Journal of Systems and Control Engineering*, 204, 33–40.
- Edge, K.A. and Johnston, D.N., 1990b. The secondary source method for the measurement of pump pressure ripple characteristics. Part 2 – Experimental results. *Proceedings of the Institution of Mechanical Engineers, Part I: Journal of Systems and Control Engineering*, 204, 41–46.
- Grادل, C. and Scheidl, R., 2013. A basic study on the response dynamics of pulse-frequency controlled digital hydraulic drives. *In: E. Barth, and A. Vacca, eds. The Bath/ASME*

- Symposium on Fluid Power & Motion Control, FPMC2013*, 6–9 October, Sarasota, Florida, paper ID: FPMC2013-4438.
- Hayward, A.T.J., 1976. A linear orifice-plate flowmeter. *Journal of Physics E: Scientific Instruments*, 9, 440–442.
- HydroLib3, 2014. <http://imh.jku.at> [Accessed 20 June 2014].
- Kogler, H., 2012. *The Hydraulic Buck Converter – Conceptual Study and Experiments*. ACCM Schriftenreihe Advances in Mechatronik, Bd. 16, Trauner Verlag, Linz.
- Kojima, E. and Ichyanagi, T., 1998. Development research of new types of multiple volume resonators. In: C.R. Burrows, and K.A. Edge, eds. *1st Bath Workshop on Power Transmission and Motion Control (PTMC 1998)*, Bath, UK, 193–206.
- Kribayashi, T., et al., 2010. Research on the attenuation characteristics of a multi-degree of freedom type Helmholtz Resonator for hydraulic systems. *Proceedings of Mechanical Engineering Congress 2010 Japan*, 7, 79–80.
- Linjama, M., 2011. Digital fluid power – state of the art. In: H. Sairiala, and K.T. Koskinen, eds. *The Twelfth Scandinavian International Conference on Fluid Power*, 2 (4), SICFP'11, 18–20 May, Tampere, Finland.
- Linjama, M., Huova, M., and Vilenius, M., 2007. On stability and dynamic characteristics of hydraulic drives with distributed valves. In: D.N. Johnston, and A.R. Plummer, eds. *Power Transmission and Motion Control (PTMC 2007)*, 12–14 September University of Bath, UK. 297–314.
- Manhartsgruber, B., 2010. The influence of transmission line dynamics on the performance of digital flow control units. *The third workshop on digital fluid power, DFP'10*, 13–14 October 2010. Finland: Tampere, 107–118.
- Mikota, J., 2001. A novel, compact compensator to reduce pressure pulsations in hydraulic systems. In: *Proceedings of ICANOV – International conference on noise, acoustics and vibration*. Ottawa, Canada.
- Ortig, H., 2005. Experimental and analytical vibration analysis in fluid power systems. *International Journal of Solids and Structures*, 42, 5821–5830.
- Pan, M., et al., 2014. Theoretical and experimental studies of a switched inertance hydraulic system. *Proceedings of the Institution of Mechanical Engineers, Part I: Journal of Systems and Control Engineering*, 228 (1), 12–25.
- Plöckinger, A., Scheidl, R., and Huova, M., 2012. Simulation and experimental results of PWM for digital hydraulics. In: A. Laamanen, and M. Linjama, eds. *The fifth workshop on digital fluid power, DFP'12*, 24–25 October, 2012. Tampere, Finland, 133–152.
- Scheidl, R., Garstenauer, M., and Manhartsgruber, B., 2000. Switching type control of hydraulic drives – a promising perspective for advanced actuation in agricultural machinery. *SAE-Technical Paper Series 2000-01-2559*, Society of Automotive Engineers.
- Scheidl, R. and Hametner, G., 2003. *The role of resonance in elementary hydraulic switching control*. *Proceedings of the Institution of Mechanical Engineers, Part I: Journal of Systems and Control Engineering*, 217, 469–480.
- Scheidl, R., Lukachev, E., and Haas, R., 2014. A hydraulic switching control concept exploiting a hydraulic low pass filter. In: L.J. De Vin, and J. Solis, eds. *The 14th mechatronics forum international conference*, 16–18 June, Karlstad, Sweden.
- Scheidl, R. and Kogler, H., 2013. Hydraulische Schaltverfahren: Stand der Technik und Herausforderungen. *Ölhydraulik und Pneumatik*, 57 (2), 6–18.
- Suzuki, K., 1991. Improving Zielke's method of simulating frequency-dependent friction in laminar pipe flow. *Journal of Fluids Engineering*, 113, 569–573.
- Viersma, T.J., 1980. *Analysis, synthesis and design of hydraulic servosystems and pipelines (Studies in Mechanical Engineering)*. Amsterdam: Elsevier.
- White, P.R.S., et al., July-Sept 1984. The development of novel linear air dampers for use in sea-wave energy converter model tests. *Transactions of the Institute of Measurement and Control*, 6 (4), 182–188.
- Zielke, W., 1968. Frequency-dependent friction in transient pipe flow. *ASME Journal of Basic Engineering*, 90 (1), 109–115.